Chapter 16

Synthesis of Functional Materials by Non-Newtonian Microfluidic Multiphase System

Yong Ren, Kai Seng Koh and Yaping Zhang

Additional information is available at the end of the chapter

http://dx.doi.org/10.5772/64521

Abstract

With increasing level of polymer solution involvement in multiphase microdevice for formation of emulsion and fabrication of functional materials, it is of paramount importance to systematically understand the relevant physics of droplet formation in non-Newtonian fluids and how the material formation process may be affected due to the complex rheological effect. The chapter aims to review and discuss the recent advances in technologies that enable fabrication and application of functional materials formed from non-Newtonian microfluidic multiphase system. Rheological behavior of polymer solutions and the mathematical models are reviewed. The influence of microstructure on rheological behavior of polymer solutions and the fundamental physical phenomena driving non-Newtonian microfluidic multiphase system are discussed. Shear thinning and viscoelastic effect on breakup dynamics and droplet formation are presented. The microfabrication process of the device and synthesis of emulsion-templated materials with potential industrial and biochemical applications are elucidated.

Keywords: non-Newtonian fluid, microfluidic, multiphase system, functional material

1. Introduction

Emulsion is mixture of two immiscible liquids, where one liquid is dispersed as droplets in another liquid that forms a continuous phase [1]. The availability of a wide range of technologies for emulsion generation and manipulation by microfluidic multiphase system has enabled the applications of microfluidics in a plethora of fields, such as fabrication of core-shell microspheres and capsules using emulsion droplets as a template for drug encapsulation and release and generation of jets as precursors of microfibers for application in wound dressing and tissue engineering. Emulsion can be formed with aqueous/oil multiphase system or all aqueous multiphase system, both of which involves the use of Newtonian fluids or non-

Newtonian fluids. In Newtonian fluids such as simple organic liquids, solutions of low-molecular-weight inorganic salts, molten metals, or salts, the shear stress at steady condition in laminar flow is linearly proportional to the shear rate, i.e., the tensors that describe the viscous stress and the strain rate are related by a constant viscosity tensor which is independent of the stress state and velocity of the flow. In contrast, non-Newtonian fluids possess such properties that flow curve of shear stress versus shear rate is nonlinear or does not pass through the origin and the apparent viscosity as defined by shear stress divided by shear rate is not constant at a given temperature and pressure, as the apparent viscosity is also influenced by shear rate, the kinematic history of the fluid element, flow conditions, or microchannel configurations. The ever-expanding applications of microfluidic multiphase technologies increasingly require the use of non-Newtonian fluids, examples of which in daily life include cement paste, chocolate, coal slurries, greases and lubricating oils, molten polymer solutions, and cosmetics and personal care products such as shampoos, shaving foams, and toothpaste. Non-Newtonian multiphase microsystem has become a subject of intense research and is widely applied in biomedical engineering, food production, and energy applications. It is hence important to understand the associated physical phenomena, in particular the way how non-Newtonian rheological effect will alter breakup dynamics and, in turn, affect droplet formation, which can be characterized by droplet shape and size, as they are closely related with droplet stability as well as optical and mechanical properties [2]. For example, the shape and size of emulsion droplets have significant impacts on the drug release kinetics when they are used as template to synthesize microcapsules or microparticles for drug delivery [3, 4]. Monodisperse droplets with precisely controlled sizes can be used to deliver an accurate dosing of contained payload such as drug, flavoring, or chemical reactants [5]. Monodispersity and size tenability are highly desired to keep droplets exhibiting constant, controlled, and predictable properties. Nevertheless, the versatility in droplet size control is challenged by complex rheological properties of non-Newtonian fluids, such as formation of undesirable satellite droplets due to bead-on-string patterns, as a result of the stretching and thinning of non-Newtonian liquid filaments. Apart from that, a number of non-Newtonian fluids such as polymeric solutions, whole blood, or protein solutions with large polymeric molecules often exhibit elastic property with shear rate-dependent viscosity due to the stretching and coiling of the polymer chains [6, 7]. Novel applications may arise from non-Newtonian rheological behaviors [8]. For instance, three-dimensional (3D) focusing of microparticles can be achieved via an approach combining inertial and elastic forces in viscoelastic solutions [9]. The elasticity of the focusing fluid can facilitate formation of smaller droplets [10].

In this chapter, we aim to summarize the main technologies for non-Newtonian microfluidic multiphase system and discuss the recent advances in technologies that enable fabricating and characterizing functional materials formed from such systems. The chapter will start with review of rheological behavior of polymer solutions followed by discussion of the fundamental physical phenomena driving non-Newtonian microfluidic multiphase system where polymer solutions are involved; non-Newtonian viscosity effect on breakup dynamics and droplet formation; the techniques employed in device fabrication; and synthesis of emulsion-templated materials. Emphasis will be placed on synthesis of functional materials from single emulsion, double emulsion, or higher order emulsions. Finally we conclude with an outlook

http://dx.doi.org/10.5772/64521

to the future of the field. This chapter is meant to familiarize readers who may be new to the field of non-Newtonian microfluidics, as well as those readers who are new to the field of synthesis of functional materials, and eventually bridge the knowledge gap between the two disciplinary fields, leading to novel approaches for design of functional materials with tailored behaviors for specific applications.

2. Rheological characteristics of polymer solutions

Polymer solutions form a class of industrially significant materials exhibiting diversity of non-Newtonian rheological properties. The system with polymer solutions exhibits a rich spectrum of interesting and complex characteristics once the polymer molecules begin to interact, entangle, and knot up with each other. For example, a macromolecule responds to external force via straightening of chains, disentangling of loose networks, uncoiling and stretching, etc., in the presence of an imposed flow or force. Brownian effects tend to randomize the flow units present in such polymeric systems. The significant factors governing the rheological behavior of a polymeric system are the molecular weight, molecular weight distribution, the structure of the molecule, their possible configurations, and the chemical composition. The use of polymer solutions in microfluidic applications requires knowledge and understanding of their complex behaviors. First, we will review classification of non-Newtonian fluids and the mathematical models. Subsequently, the influence of microstructure on rheological behavior of polymer solutions will be discussed.

For an incompressible Newtonian fluid at steady condition in simple shear flow case where a thin layer of a fluid is contained between two parallel planes which have surface area of A and are parted by a distance dy, a shear by the application of a force F is exerted on the fluid, the shear rate may be expressed as the velocity gradient in the direction perpendicular to that of the shear force, and velocity vector has only one component along x direction with magnitude varying only in y direction, the shear will be balanced by an equal and opposite internal frictional force in the fluid:

$$\frac{F}{A} = \tau_{yx} = \eta\left(-\frac{dV_x}{dy}\right) = \eta\dot{\gamma}_{yx} \tag{1}$$

where τ represents shear stress, η the viscosity of fluid of interest, V the velocity, and $\dot{\gamma}$ the shear rate. The first subscript indicates the direction normal to that of shearing surface, while the second subscript refers to the direction of the force and the flow. The negative sign on the right hand side of Eq. (1) indicates that τ is a measure of the resistance to motion. Viscosity η only depends on material of interest, as well as temperature and pressure.

The shear stress for more general 3D case of an incompressible Newtonian fluid may be expressed for the x plane oriented normal to the x direction as follows [11]:

$$\tau_{xx} = -2\eta \frac{\partial V_x}{\partial x} + \frac{2}{3}\eta\left(\frac{\partial V_x}{\partial x} + \frac{\partial V_y}{\partial y} + \frac{\partial V_z}{\partial z}\right) \tag{2}$$

$$\tau_{xy} = -\eta\left(\frac{\partial V_x}{\partial y} + \frac{\partial V_y}{\partial x}\right) \tag{3}$$

$$\tau_{xz} = -\eta\left(\frac{\partial V_x}{\partial z} + \frac{\partial V_z}{\partial x}\right) \tag{4}$$

Similar sets of equations can be developed for the forces acting on the y and z planes. In each case, there are two shearing components and one normal component. The nine stress components of a fluid element are shown in Figure 1. $\tau_{xy}=\tau_{yx}$,,nd $\tau_{yz}=\tau_{zy}$, because of the equilibrium of a fluid element. Each component of normal stress consists of two components: isotropic pressure and a contribution from flow depending on fluid type:

$$\begin{aligned} P_{xx} &= -p + \tau_{xx} \qquad (\mathrm{a}) \\ P_{yy} &= -p + \tau_{yy} \qquad (\mathrm{b}) \\ P_{zz} &= -p + \tau_{zz} \qquad (\mathrm{c}) \end{aligned} \tag{5}$$

where p denotes the isotropic pressure and τ_{xx}, τ_{yy}, and τ_{zz} represent deviatoric normal stresses of Newtonian fluids or extra stresses of non-Newtonian fluids. For an incompressible Newtonian fluid, it is given by

$$p = -\frac{1}{3}\left(P_{xx} + P_{yy} + P_{zz}\right) \tag{6}$$

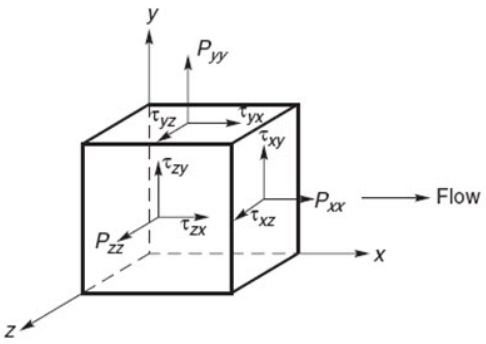

Figure 1. Stress components in 3D flow.

http://dx.doi.org/10.5772/64521

Based on Eqs. (5)–(6), it can be derived that

$$\tau_{xx} + \tau_{yy} + \tau_{zz} = 0 \tag{7}$$

For a Newtonian fluid in simple shear flow,

$$\tau_{xx} = \tau_{yy} = \tau_{zz} = 0 \tag{8}$$

Newtonian fluid thus not only possesses a constant viscosity but also satisfies the condition of Eq. (8). Boger fluids possess constant shear viscosity but do not conform to Eq. (8); thus they must be treated as non-Newtonian fluids. Three types of non-Newtonian fluids are ubiquitously applied and widely investigated [12–14]: (1) time-independent fluids (it can be further subdivided into three types including shear thinning, viscoplastic thickening, and shear thickening), (2) time-dependent fluids, and (3) viscoelastic fluids. Since most polymer solutions possess shear-thinning and viscoelastic behavior, only these rheological properties will be discussed in this chapter.

2.1. Shear thinning

Pseudoplasticity or shear-thinning behavior is characterized by an apparent viscosity which decreases with increasing shear rate. However, most shear-thinning polymer solutions and melts exhibit Newtonian behavior at very low and very high shear rates. The values of the apparent viscosity at very low and high shear rates are known as the zero shear viscosity, η_0, and the infinite shear viscosity, η_∞, respectively. Thus, the apparent viscosity of a shear-thinning fluid decreases from η_0 to η_∞ with increasing shear rate. As molecular weight of the polymer is smaller, or its molecular weight distribution becomes narrower, or as polymer concentration drops, it will extend the range of shear rate over which the apparent viscosity is constant. A selection of the more widely used viscosity models is summarized here.

i. *The power law or Ostwald de Waele model*

The relationship between shear stress and shear rate for a shear-thinning fluid can often be approximated by a straight line over a limited range of shear rate (or stress) plotted on double logarithmic coordinates. This part of the flow curve can be modeled by power law or Ostwald de Waele expression in the following form:

$$\tau = m\dot{\gamma}^n \tag{9}$$

so the apparent viscosity is thus given by

$$\eta = \frac{\tau}{\dot{\gamma}} = m\dot{\gamma}^{n-1} \tag{10}$$

In these equations, *m* and *n* are two empirical curve-fitting parameters and are known as the fluid consistency coefficient and the flow behavior index, respectively. The fluid exhibits shear-thinning properties, Newtonian behavior, and shear-thickening behavior when n<1, n=1, and n>1, respectively. The smaller the value of *n,* the greater is the degree of shear thinning. This model applies for only a limited range of shear rates and therefore the fitted values of *m* and *n* will depend on the range of shear rates considered. The zero and infinite shear viscosities are not taken into account.

ii. *The Carreau viscosity equation*

The Carreau viscosity model incorporates both upper and lower limiting viscosities η_0 to η_∞ and is given by

$$\frac{\eta-\eta_\infty}{\eta_0-\eta_\infty}=\left(1+\left(\lambda\dot{\gamma}\right)^2\right)^{(n-1)/2} \tag{11}$$

where *n* and λ are two curve-fitting parameters. This model can describe shear-thinning behavior over wide ranges of shear rates but only at the expense of the added complexity of four parameters.

iii. *The Cross viscosity equation*

This model has also gained wide acceptance and, in simple shear, is written as

$$\frac{\eta-\eta_\infty}{\eta_0-\eta_\infty}=\frac{1}{1+k\dot{\gamma}^n} \tag{12}$$

This model can be reduced to the Newtonian fluid behavior as k approaches 0 or the power law model as shown in Eq. (10) when $\eta \ll \eta_0$, and $\eta \gg \eta_\infty$.

2.2. Viscoelastic fluids

Such substances exhibit characteristics of both ideal fluids and elastic solids and show partial elastic recovery after deformation, as they have the ability to store and recover shear energy. Examples include polymer melts, polymer and soap solutions, and synovial fluid. The shearing motion of a viscoelastic fluid gives rise to the first and second normal stress differences N_1 and N_2, expressed in terms of two coefficients, ψ_1 and ψ_2, which for 1D flow are defined by

$$\begin{aligned}\psi_1&=\frac{N_1}{\dot{\gamma}_{yx}^{\ 2}} \quad \text{(a)}\\ \psi_2&=\frac{N_2}{\dot{\gamma}_{yx}^{\ 2}} \quad \text{(b)}\end{aligned} \tag{13}$$

http://dx.doi.org/10.5772/64521

At very low shear rates, the first normal stress difference, N_1, is normally proportional to the square of shear rate, and N_1 is larger than the shear stress τ at the same value of shear rate. The ratio of N_1 to τ is often taken as a measure of how elastic a liquid is. When recoverable shear, $N_1/2\tau$, is greater than 0.5, it indicates a highly elastic behavior of the fluid. The two normal stress differences are used to categorize a fluid either as purely viscous (N_1 =0) or as viscoelastic, and the magnitude of N_1 in comparison with τ_{yx}, is often used as a measure of viscoelasticity. N_2 is usually small, with maximum values not exceeding 20% of N_1 and with an opposite sign to N_1. Measurement of N_2 is difficult and can be done using a special cone-plate apparatus [12]. N_1 is responsible for some spectacular phenomena, such as the Weissenberg effect [6]. The measurement of N_1 can be conducted by commercial rotational rheometers. For the flow of polymer solutions in porous media, extensional effects are often encountered and the fluid is stretched as the extent and shape of the flow passages change. Elongational viscosity η_E is defined as

$$\eta_E = \frac{P_{xx} - P_{yy}}{\dot{\varepsilon}} = \frac{\tau_{xx} - \tau_{yy}}{\dot{\varepsilon}} \tag{14}$$

where $\dot{\varepsilon}$ is the elongational rate. Elongational viscosity can only be directly measured with devices like capillary breakup extensional rheometer [15]. The Trouton ratio, T_r, is defined as

..

$$T_r = \frac{\eta_E}{\eta} \tag{15}$$

For inelastic isotropic fluids, T_r =3 for all values of $\dot{\varepsilon}$ and $\dot{\gamma}$, and any deviation from the value of 3 indicate the existence of viscoelasticity. The Maxwell model is one of widely used linear viscoelastic models; a mechanical analogue of this model is obtained by series combinations of a spring and a dashpot. Combining the Hooke's law of elasticity and Newton's law of viscosity, one can obtain

$$\tau + \lambda \dot{\tau} = \eta \dot{\gamma} \tag{16}$$

where $\dot{\tau}$ is the time derivative of τ, η is the viscosity of the dashpot fluid, and λ (=μ/ G) is the relaxation time, which is a characteristic of the fluid. A more solid-like behavior is obtained by considering the so-called Voigt model which is represented by the parallel arrangement of a spring and a dashpot. The fluid total extra stress (τ_t) is given as the sum of an incompressible solvent contribution having a viscosity coefficient η_s and a polymer/additive stress contribution τ_p, as

$$\tau_t = 2\eta_s\left(II_{D,}III_D\right)D + \tau_p \tag{17}$$

The solvent viscosity coefficient in Eq. (18) has been made to depend on the second and third invariants ($II_{D,}III_D$) of the rate of deformation tensor D, which is defined as

$$D = \frac{1}{2}\left(\nabla V + \nabla V^T\right) \tag{18}$$

For viscoelastic fluids, η_s is set to zero for polymer melts or to a nonzero constant when dealing with a polymer solution based on a Newtonian solvent. Flows in viscoelastic solutions are governed by the Deborah number, De; the Weissenberg number, Wi; and the elasticity number, El. The Deborah number is defined as the ratio between the relaxation time of the fluid (λ) and the time of observation of the flow (t_f), such as the duration of the unsteady part of a flow:

$$De = \frac{\lambda}{t_f} \tag{19}$$

The Weissenberg number is defined as the product of the relaxation time and a characteristic rate of deformation of the flow (V/L) and quantifies the nonlinear response of the fluid

$$Wi = \lambda\frac{V}{L} \tag{20}$$

while El represents the ratio between elastic and inertial effects

$$El = \frac{Wi}{\mathrm{Re}} = \frac{\lambda\eta}{\rho L^2} \tag{21}$$

where ρ is the density. High Wi may lead to onset of elastic instabilities of viscoelastic fluids, even under creeping flow conditions. For instance, fluids with large polymeric molecules often exhibit elastic behavior due to the stretching and coiling of the polymeric chains, which significantly enrich flow behavior [6].

2.3. Microstructure effect to rheology of polymers

The zero shear viscosity of most polymeric systems increases linearly with the molecular weight below a critical value of the molecular weight, which denotes the onset of entanglement. The zero shear viscosity scales with molecular weight more significantly with the molecular weight above this value. The rheology of polymers is also affected by the nature of chains

http://dx.doi.org/10.5772/64521

whether these are rod-like or coils and springs. For example, the charge-induced repulsive forces along the polymer chain will straighten the convoluted chain and impart some features of rod-like systems in the case of a polyelectrolyte in a weak electrolyte solution. Long molecules are normally randomly oriented at low shear rate, while the molecules become aligned along the direction of flow when increasing the shear rate progressively. The rheological properties are also extremely sensitive to chemical composition. In polymer industry, it is a common technique for producing new rheological properties by adding fillers. The extent of modifications of viscosity-shear rate curves for filled systems depends upon the size and shape of fillers as well as concentration [16]. Blending of polymers can also be used to improve rheological characteristics as compared to that of the constituents. Such a blend may exhibit viscosity larger than that of its constituents. Another way to obtain improved mechanical properties is to create a block copolymer. Such a molecule has long sequences of one type of polymer connected to long sequences of another polymer and exhibits elastic behavior at room temperature and ease of flow at high temperatures, leading to wide range of applications. Surfactant systems also constitute an important class of industrial materials which exhibit complex rheological behavior. The surfactant molecules have hydrophobic tails and hydrophilic heads. When a surfactant like soap or detergent is added to water with concentration beyond a critical value, micelles comprising several molecules begin to form. The formed structures have temporary and loose networks which are continuously broken down and reformed. The shape of micelles includes spherical, rod-like, lamellar sheets and lamellar droplets, which are subject to several parameters, including temperature, the shape of the surfactant molecule, and electrolytic nature of water.

3. Non-Newtonian viscosity effect on breakup dynamics and droplet formation

Emulsion droplets can be passively formed by fluid instabilities using four of the most prevalent microfluidic geometries found from literature: coaxial [17], flow focusing [18], T junction [19], and step emulsification [20]. The dynamics of the droplet formation in microsystem can be characterized by a transition from dripping to jetting regime, governed by the Weber number of the dispersed phase, We_{in}, defining the ratio of inertial force to surface tension and the capillary number of the continuous phase, Ca_{out}, defining the ratio of viscous force to surface tension:

$$We_{in} = \frac{\rho_{DP} L V_{DP}^{\ 2}}{\sigma} \tag{22}$$

$$Ca_{out} = \frac{\eta_{CP,0} V_{CP}}{\sigma} \tag{23}$$

where L refers to the characteristic dimension of the microsystem and $\eta_{CP,0}$ is the apparent viscosity of the non-Newtonian fluid of continuous phase. The subscript "0" refers to zero

shear rate when a shear-dependent fluid is used, and DP refers to dispersed phase. Formation regime of droplets and its transition are also studied in glass capillary device, where dripping regime and jetting regime are dominant and their transition depends on both capillary number and Weber number [21]. Droplet formation occurs at small Ca_{out} and We_{in} when flows are dominated by surface tension, while jetting forms at large Ca_{out} or We_{in} when the viscous stress or the inertial force on the droplet is large enough to overcome surface tension. Droplets are generated after breakup of a jet at some distance downstream in this regime. Emulsification processes using T- or Y-shaped junctions in poly(dimethylsiloxane) (PDMS) microfluidic systems have been applied for bioassays or drug delivery. The scaling laws of droplet formation by cross flow in T-junction devices were investigated, leading to discovery of three droplet formation patterns: (1) at Ca<0.002 (plug flow is dominant when squeezing regime occurs because n cross-flow shear is low and cannot rupture the disperse phase into drops), (2) at 0.01<Ca<0.3 (droplets are formed with a size comparable to channel cross-sectional dimension in dripping regime because shear force is large enough to cause breakup at the T junction), and (3) transition regime between the two. Simple models for dimension prediction of droplets and plugs as functions of reciprocal Ca were suggested for the squeezing and dripping regimes, respectively [22]. The formation of plug-shaped droplets and mixing in the microchannel with a T junction were studied [23]. While the dynamics of droplet breakup has been systematically investigated in Newtonian fluids, the validity of the understanding has not been adequately confirmed in non-Newtonian fluid systems. With increasing level of polymer solution involvement, systematic understanding of the relevant physics of droplet formation in non-Newtonian fluids has become particularly important. The complex rheological properties of non-Newtonian fluids also affect breakup dynamics and furthermore challenge the versatility in droplet size control. For example, the stretching and/or thinning of non-Newtonian liquid filaments will lead to the formation of "bead-on-string" patterns, as the interface pinch-off is greatly hindered by the polymers' tendency to recover their equilibrium state [24, 25]. These beads can subsequently become undesirable satellite droplets, increasing the polydispersity of the resultant droplet population. These examples attest to the need for a comprehensive understanding of the role of non-Newtonian viscosity effect in droplet formation using microfluidic systems. In this section, the non-Newtonian viscosity effect on the mechanism of droplet breakup, the characteristics of droplets such as final droplet size, and the frequency of droplet formation will be presented and discussed. We will focus on shear-thinning and viscoelastic fluids in different types of multiphase microsystems such as glass capillary device and planar PDMS device.

3.1. Shear-thinning effect

3.1.1. Glass microcapillary device

The dripping-to-jetting transition under various flow conditions in a Newtonian/shear-thinning multiphase microsystem was characterized [17]. A numerical model of the microcapillary co-flow device has been developed with a Newtonian fluid injected in a cylindrical capillary as the dispersed phase at a constant average velocity V_{DP} and a non-Newtonian outer phase injected through the coaxial square capillary as the continuous phase at a constant average

http://dx.doi.org/10.5772/64521

velocity V_{CP} (see Figure 2). The dispersed phase was silicon oil, while the continuous phase was 2% (w/v) aqueous solution of sodium rboxymethyl cellulose (CMC) (Mw=250,000 Da, DS=1.2), which is a pseudoplastic fluid and demonstrates shear-thinning behaviors with its apparent viscosity defined by Eq.(12) using Cross model. The breakup dynamics in a non-Newtonian fluid system was compared with a Newtonian fluid system at the same Weber number and capillary number using the same microdevice. For the Newtonian two-phase flow, silicone oil was also used as the dispersed phase, while 17% (w/v) aqueous solution of polyethylene glycol (PEG) (Mw=8,000 Da) was used as the continuous phase. The dispersed phase was purged out of the orifice (see Figure 3a) with a droplet growing in size and moving downstream while still connecting with the fluid neck through the orifice via a filament (see Figure 3b). The filament gradually became thinner (see Figure 3c) and finally broke up into a droplet (see Figure 3d). The process was repeated afterward. The interface between the two phases was tracked and compared with experimental measurements with reasonable agreement.

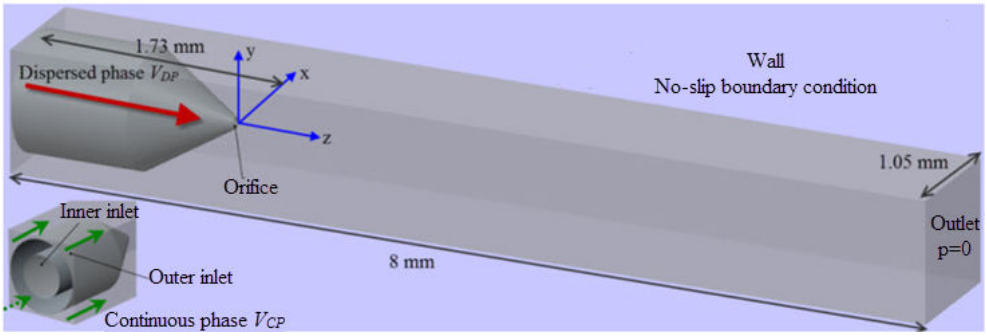

Figure 2. Schematic of the computational domain of multiphase microfluidic system. The closeup view of meshing of nozzle and inlets is shown in inset. Reproduced from Ref. [17] with permission from the Royal Society of Chemistry.

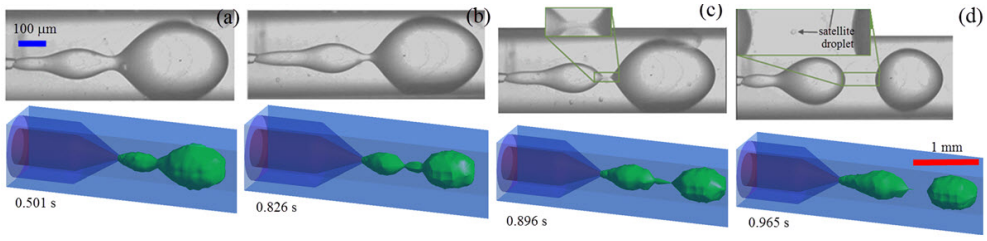

Figure 3. Time-lapse images of jet deformation and droplet formation from simulation (upper one in each sub-figure) and experiments (lower one in each sub-figure) using a Newtonian/shear-thinning two-phase co-flow system (silicon oil as dispersed phase and CMC solution as continuous phase). The blue and red scale bars are applicable for the experimental and simulation results, respectively. (a) The dispersed phase is purged out of the orifice; (b) the main droplet is connected with the fluid neck via a thin filament; (c) the filament becomes even much thinner; (d) satellite droplet occurs after breakup of the jet. Reproduced from Ref. [17] with permission from the Royal Society of Chemistry.

Droplet size scales inversely with the capillary number of the continuous phase in a monotonous fashion in the Newtonian/Newtonian two-phase system [26]. In contrast, the correlation between the droplet size and the capillary number in the Newtonian/shear-thinning two-phase system is different. As Ca_{out} and the shear rate of continuous phase increase, the viscosity of continuous phase is reduced for shear-thinning fluids such as CMC, leading to formation of larger droplets [27]. However, when Ca_{out} increases beyond a critical value, the viscous drag can overcome the surface tension effects that would otherwise minimize the stretching of the fluid neck by drawing the fluid interfaces closer to the orifice. The fluid neck becomes stretched and elongated at high Ca_{out}, fluid neck will subsequently become thinner, the shear rate of the continuous phase starts to decrease, the viscosity of continuous phase will increase for a shear-thinning fluid, and eventually the droplet undergoes size reduction beyond a critical Ca_{out}.

3.1.2. PDMS device

The effects of the generalized power law coefficient, the power law exponent and the yield stress on the mechanism of drop breakup, final drop size, and frequency of drop formation were studied using 3D volume of fluid (VOF) model in multiphase flows in T-shaped microchannel where the fluids are Newtonian/power law and Newtonian/Bingham [28]. The pressure implicit with splitting of operators (PISO) algorithm was used in the transient calculations for droplet generation and deformation. The technique of piecewise-linear interface construction (PLIC) [29] that satisfies the accuracy of the surface tension calculations was adopted in this numerical model. The droplet diameter decreased and frequency increased with $n \leq .\ 0.9$ and $n \geq .\ 0.92$. The products of η_{cp}. and $\dot{\gamma}$ did not change much from K = 0.0011 to 0.0106 Pa s. For Bingham fluid, the droplet extension increased significantly as yield stress became larger. A plug-flow region was found in flows of Bingham fluids, and the width of the region was proportional to the yield stress. With a Bingham fluid as the continuous phase, an obvious transition period was found before the droplets can be formed steadily. During this transition period, droplets coalescence was observed. Microdroplet formation in different channel geometries has been studied. For instance, the formation of droplet from an aperture was investigated under the cross-flow conditions in microchannel emulsification process [30], where an oil phase was dispersed into shear-thinning continuous-phase fluid through a microchannel wall made of apertured substrate. The dispersed oil phase first grew to a jetlike deformed droplet, indicating that the net shear effect on the droplet surface in the flow direction of a non-Newtonian continuous phase is stronger than that in Newtonian flow. The detached droplet had a diameter less than half of the droplet size in the Newtonian flow case, showing a drastic reduction in the droplet size by the non-Newtonian effect in typical dripping regime, due to higher shear stress near the wall. Simulations of a droplet passing through an axisymmetric contraction were performed using VOF algorithm [31]. When the disperse phase was shear thinning, the local viscosity of the droplet decreased as it entered the contraction, remained low while within the contraction, and increased as it exited. When the continuous phase was shear thinning and the dispersed phase was Newtonian, the droplets tended to deform less than their shear-thinning counterpart when entering the contraction.

http://dx.doi.org/10.5772/64521

3.2. Viscoelastic effect

3.2.1. Glass microcapillary device

The flow patterns at different ratios of flow rate with viscoelastic continuous phase of 5% w/v PAA solution and dispersed phase of silicon oil were characterized [17]. The elastic forces from viscoelastic continuous phase help to overcome interfacial tension and thus facilitate transition to jetting at smaller magnitudes of the viscous forces. Droplets adopted a spherical or nearly spherical shape in Newtonian/Newtonian or Newtonian/shear-thinning multiphase microsystem, while the droplets experienced significant deformation in the viscoelastic non-Newtonian continuous phase, because elasticity of the suspending liquid can facilitate the deformation of the Newtonian droplets [32]. For instance, the droplets adopted an elliptical shape after breakup and relaxed into pointed shapes. Droplets became more pointed as the radius decreased and the flow rate ratio increased before it transitioned to the jetting regime. The degree of droplet deformation increased, leading to formation of droplets with more pointed shape, when elastic effect became more pronounced at higher Weissenberg number. This work helps to understand how the complex rheology behavior of viscoelastic fluid can influence the breakup dynamics and droplet formation in multiphase microfluidic system when glass capillary device is used.

3.2.2. PDMS device

Highly controlled shear in viscoelastic media can lead to droplet rupturing down to a unique size and the shear-thinning nature enhances the monodispersity [33]. The droplet formation and breakup dynamics of elastic and Newtonian fluids in T-shaped microchannels for continuous phase were investigated [34]. For both cases, reduction in droplet size was found when cross-flow shear force was increased via increase of viscosity ratio of continuous phase to dispersed phase. For non-Newtonian case, after the droplet grew to a large enough size and was pushed downstream by the cross-flow, dispersed-phase filament was formed between the junction and the connected droplet. The filaments were stretched at two different rates and broke up into secondary smaller droplets. A critical Ca number existed for the inception of monodisperse secondary drops. The obvious presence of the filament during the drop detachment process of these elastic fluids when compared to its Newtonian counterpart shows that fluid elasticity played an important role in resisting drop pinch-off, and the presence of elasticity created a significant difference in drop formation dynamics, while this contributed little to the final drop size and drop productivity. The morphology of droplets was determined by polymer molecular weight and viscosity ratio. A slight reduction in primary drop size is expected with increasing levels of elastic stress within the filament, as the mass of fluid within the filament between two primary drops is excluded from effectively draining into the primary drops at either end of the filament. Analysis of the filament dynamics during the drop detachment stage revealed that there are two distinct regions: a pre-stretch region and an exponential self-thinning region. The effect of viscoelasticity of drop and medium on drop deformation was investigated, and the strategy to control the drop shape was proposed [35]. When a Newtonian drop was suspended in a viscoelastic medium, in the narrow channel

region, ellipsoid-like droplet was found. In contrast, droplet normally adopted bullet-like shape in a Newtonian/Newtonian microsystem. When a viscoelastic drop was suspended in Newtonian medium, the drop swelling extent to the cross-stream direction was enhanced at the outlet of the channel, due to the normal stress difference developed in the viscoelastic fluid.

4. Synthesis of functional materials using microfluidics

4.1. Fabrication of microfluidic emulsification system

The most common microfabrication methods for creating microfluidic devices are photolithography and soft lithography. Studies in optimizing these techniques have been extensively reported [36–40]. Photolithography actually refers to the transfer of a pattern of chromium on a hard material such as glass or silica plate and is known as the most important step in the microfabrication process. The whole process of photolithography involves substrate cleaning, photolithography, metal deposition and wet/ dry etching [41]. Silicon wafer is initially heated to a temperature of 150 °C to remove any moisture that may be present on the surface. Contaminant on the surface of silicon wafer can be removed by cleaning procedure [42]. After the cleaning process, silicon wafer is spin coated with a thin and uniform layer of photoresist. The silicon wafer along with the photoresist is then placed into the ultraviolet (UV) exposure machine for alignment and exposure. The exposure of photoresist toward UV light triggers chemical reaction; thus the exposed photoresist can be removed by a solution aimed to remove unreacted photoresist. The geometric pattern can be defined onto the silicon wafer by either positive photoresist or negative photoresist. Positive photoresist becomes soluble upon exposure whereas the unexposed regions become soluble when negative photoresist is used [43]. Soft lithography is a low-cost technique to replicate the microchannel pattern using the master mould generated with photolithography technique. In most of the applications, PDMS is the preferred elastomeric materials to be used as the patterned replica which transfer the original pattern of a master by molding or printing. The flexibility of the PDMS replicas allows patterning on nonplanar structures through micro-contact printing or micro-molding. As compared to chromium mask, film masks with similar pattern not only cost 20–100 times cheaper but also with a shorter production time. The subsequent process is very similar to the photolithography process with the only difference in which the negative replica is generated by casting an uncured prepolymer of PDMS against the geometry design [36]. However, these techniques require sophisticated instrumentation and clean room that sometimes are not readily available. Consequently, rapid yet low-cost prototyping technology, as a result of impressive development of microfabrication process aimed at reducing the fabrication interval and cost needed in conventional microfabrication processes such as xurography, was proposed to construct the devices [44, 45]. In addition, most of these techniques do not require clean-room facilities as well as sophisticated steps to produce high-quality and long-lasting microfluidic devices [46]. Xurography utilized cutting plotter with a 10 μm resolution that can directly create microstructures without photolithographic process or chemicals [47]. The design pattern was cut onto an adhesive vinyl film. This was followed by removal of undesired portions of film using a pin/ blade. The remaining film with desired design was then transferred onto a substrate, i.e., transparent plastic with the aid of the application tape to prevent

http://dx.doi.org/10.5772/64521

deformation of the design. The transparent plastic along with the designated film was then used to create an epoxy master mould in order to produce replicas of PDMS device. Although xurography does not possess high resolution as compared to standard lithography techniques, the accuracy of this method was falling within 10 μm of drawn dimensions and the feature variability was less than 2 μm [47].

4.2. Synthesis of particles using single-emulsion template

The ability to form droplets with a microfluidic device allows one to structure fluids to disperse a continuous fluid into a series of equally sized liquid spheres. These spheres can then be solidified to produce particles of the same size and shape. Monodisperse microgels consisting of cross-linked network of poly(N-isopropylacrylamide) (PNIPAm) can be formed from single emulsion (see Figure 4) [48, 49]. Such PNIPAm microgels swell and shrank reversibly in response to changes in temperature. The size change occurred around 32°C, which is close to the human body temperature. Hence, these microgels have been extensively evaluated for controlled delivery of water-soluble drugs. Low polydispersity of PNIPAm microgels is desirable for drug delivery applications as it could lead to narrow distribution of drug loading levels and uniform release kinetics. Lipids or hydrocarbons are known as natural choice of the shell material as most of them are solid at room temperature, thus enabling the robust encapsulation under ambient conditions [50].

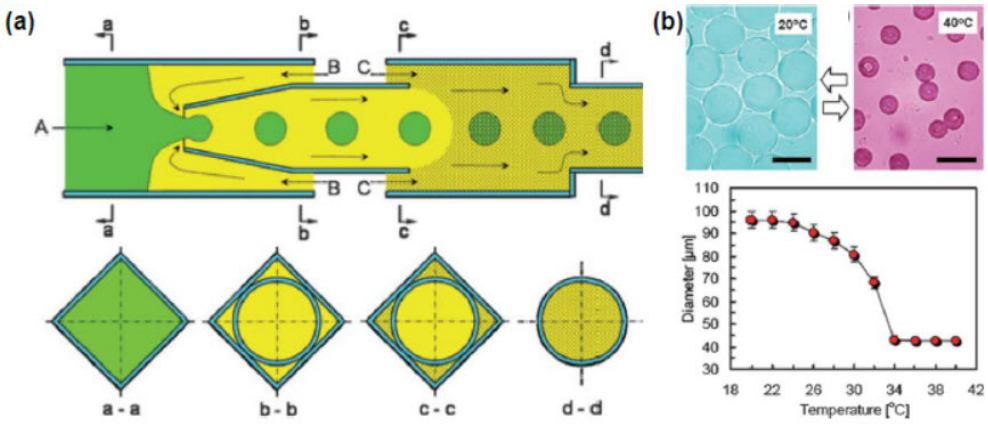

Figure 4. (a) Schematic illustration of a capillary-based microfluidic device for fabricating monodisperse PNIPAm microgels. Fluid A is an aqueous suspension containing the monomer, cross-linker, and initiator; fluid B is oil, and fluid C is the same oil as fluid B but contains a reaction accelerator that is both water and oil soluble. The accelerator diffuses into the drops and polymerizes the monomers to form monodisperse microgels. Cross-sectional views at different points along the device length are shown in the second row. Reproduced with permission from [48]. Copyright (2007) by Wiley-VCH Verlag GmbH & Co. KGaA. (b) Size change of PNIPAm microgels in water triggered by changing the temperature. The scale bar in Panel b denotes 100 μm. Reproduced with permission from [49]. Copyright (2008) by the Royal Society of Chemistry.

A demonstration of the fabrication of monodisperse colloidosomes, microcapsules with a shell composed of tightly packed colloidal particles, has been made using colloidal PNIPAm

microgels as building blocks [51]. An aqueous suspension of amine-functionalized sub-micrometer-sized PNIPAm microgels was emulsified in an oil capsule using a single-emulsion microfluidic device. Prior to emulsification, a small amount of glutaraldehyde was added to the aqueous mixture. The colloidal PNIPAm microgels assembled at the oil-water interface within the emulsion droplets due to the presence of hydrophobic isopropyl groups and hydrophilic acrylamide groups. Glutaraldehyde molecules, owing to their two reactive sites each, served as connecting links between the amine-functionalized microgels through an amine-aldehyde condensation reaction. Colloidosomes were formed via interlinking of the microgels at the oil-water interface, as shown in Figure 5a. The colloidosomes exhibited similar thermosensitive behavior with the constituent microgels. The diameter of the colloidosomes decreased by 42%, roughly equivalent to an 80% decrease in volume, when the temperature was higher than the phase-transition temperature of PNIPAm (see Figure 5b). Such material is thus very promising in applications that require targeted pulsed release of active materials.

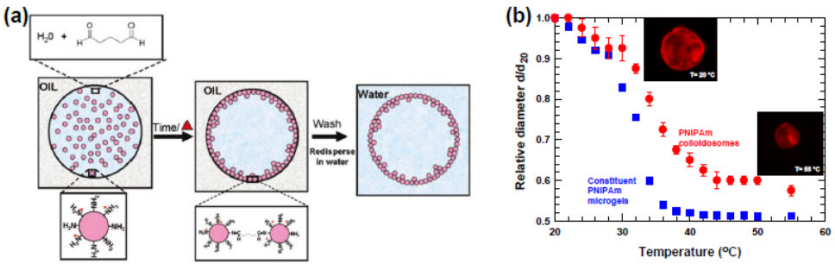

Figure 5. (a) Schematic representation of a technique used for fabricating colloidosomes using PNIPAm microgel particles as building blocks and emulsion droplets as templates. (b) Equilibrium size change of PNIPAm colloidosomes and the constituent PNIPAm microgels. Colloidosomes were dispersed in water and heated from 20 to 50 °C in fixed increments of 2 °C and then to 55 °C. Images were captured after allowing the sample to equilibrate for 30 min at each temperature. The sample was then cooled down to 20 °C using the same temperature steps. Size-change data of the constituent PNIPAm microgels over the same temperature range were collected using dynamic light scattering. Adapted and reproduced with permission from [51]. Copyright (2010) by American Chemical Society.

4.3. Synthesis of particles using double and higher order emulsion template

Double emulsion can also be used to template structures, but these structures have more elaborated shapes. To illustrate this templating process, thermoresponsive PNIPAm was chosen as the matrix polymer to obtain environmentally sensitive microgel particles with microshell structure [52]. To form the pre-microgel droplets, an aqueous microgel precursor solution was emulsified in a continuous oil phase. Pre-microgel droplets were loaded with inner droplets of another oil in the formation process, thereby creating a shell structure, as shown in Figure 6a. After droplet formation, the shell was gelled by thermal monomer polymerization by photochemical polymer-analogous gelation, yielding uniform PNIPAm microshells as shown in Figure 6b. Operating the device with different flow rates can produce shells with two cores, as shown in Figure 6c.

Colloidosomes of diblock copolymers have been fabricated by combining water-in-oil-in-water (W/O/W) droplet encapsulation and dewetting transition in a microcapillary device [53].

http://dx.doi.org/10.5772/64521

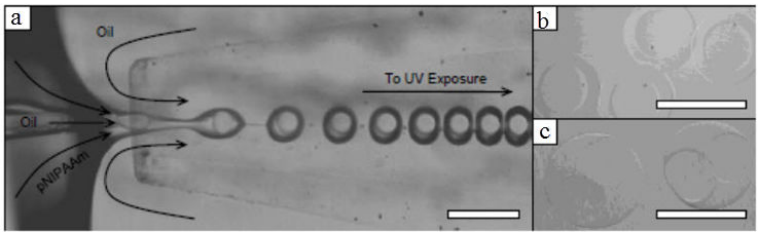

Figure 6. Microfluidic production of hollow microgel shells. (a) A glass microcapillary device is used to create an oil-water-oil double emulsion with a semidilute solution of cross-linkable pNIPAAm as aqueous phase. Subsequently, these droplets are cured by UV exposure as they flow through a delay capillary a few centimeters downstream (not shown). (b) pNIPAAm microshells obtained from the experiment in Panel A. (c) Double-core microshells obtained upon slight variation of the flow rates in the experiment. All scale bars denote 200 μm. Reproduced with permission from [52]. Copyright (2010) by the Royal Society of Chemistry.

The properties of the colloidosomes, for example, membrane thickness, mechanical response, permeability, and thermal stability, can be tuned by varying the block ratios of the block copolymers and the homopolymer [54]. Multicompartmental polymersomes can be generated based on encapsulation of a controlled number of single polymersomes through a reinjection method [55]. Besides using glass capillary devices, double emulsions can be formed in PDMS device. This can be achieved using two drop makers in series [56–58]. The first drop maker produced the inner drops, which were fed into the inlet of the second drop maker, which produced the outer drops. This type of double emulsification can be achieved using either cascading T junctions or flow-focus drop makers. Generally, serial flow-focus devices are used, because the symmetric injection of the middle and continuous phases helps prevent wetting of the drops on the channels, making the formation more robust. In addition to geometrical considerations like this, it is also necessary to control the wetting properties of the devices; however, in contrast to single-emulsion formation in which only uniform wetting is required, spatially patterned wettability is required in double or higher order multiple emulsification.

Wettability determines the type of emulsion formed in PDMS device channel: oil-in-water emulsions are formed in hydrophilic channels, while water-in-oil emulsions are formed in hydrophobic channels. The need to spatially control the wettability in PDMS devices has stimulated techniques to spatially modify device surface properties. With a photo-patterning approach, the devices were filled with a solution that only reacts with the channels under exposure to intense UV light [58]. Since the UV beam can be shaped using holes, slits, and lenses, this approach allows for the creation of complex wettability patterns. However, in the case of double-emulsion devices, only a very simple wettability pattern is needed, and the added complication of having to align the photo-pattern with the microchannels can make this approach unattractive in these instances. For the simple patterns needed for these devices, a different approach is available that trades versatility in the pattern shape for simplicity in the treatment process. This flow-patterning technique controls wettability by introducing a reactive solution into select portions of a device and preventing it from going using the flow of an inert blocker solution [59]. The reactive solution changes the wettability only in the treated

regions, while the untreated areas retain their default wettability. By controlling how the solutions are injected, wettability patterns for W/O/W or O/W/O double emulsions can be created.

One of the advantages of PDMS-based microfluidics is the ability to customize the devices to construct sophisticated channel networks. High-order multiple emulsions can be formed by scaling up device complexity. A high-order multiple emulsion is the logical continuation of a double emulsion to larger numbers of nested droplets: A triple emulsion is a double emulsion encapsulated within a droplet, while a quadruple emulsion is merely a triple emulsion inside yet another droplet. As shown in Figure 7a, double emulsions can be formed by addition of another droplet maker; together also pattern wettability, so that the inner drops were encapsulated within larger drops of an immiscible phase (see Figure 7b) [60]. The design can be further improved to make higher order emulsions such as triple, quadruple, and quintuple emulsions by addition of third, fourth, and fifth junctions, as shown in Figure 7c–e, respectively.

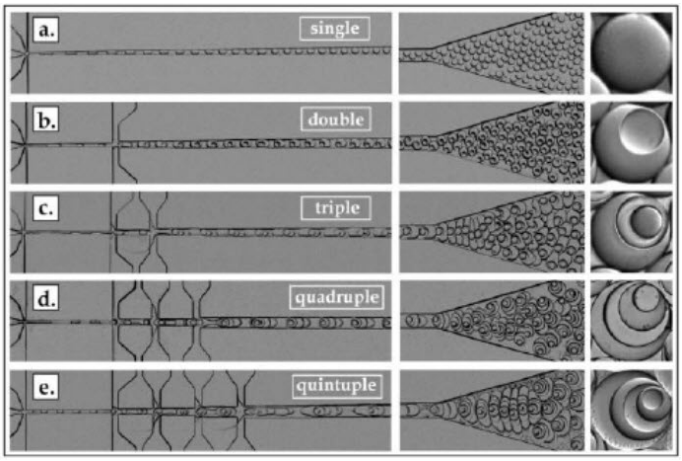

Figure 7. Serial drop maker arrays used to form multiple emulsions. A single-emulsion droplet takes one drop maker to create (a), whereas double, triple, quadruple, and quintuple emulsions take two, three, four, and five drop makers in series to create, (b), (c), (d), and (e), respectively. The wettability of the multiple emulsion devices has been patterned so that it inverts between hydrophilic and hydrophobic from one junction to the next. Reprinted with permission from [60]. Copyright (2009) by Wiley-VCH Verlag GmbH & Co. KGaA, Weinheim.

A number of polymer solutions cannot be used to synthesize particles in microfluidic devices, as challenged by their non-Newtonian properties. For instance, lipid melts such as coco glycerides tend to be viscous and stick to channel surfaces because of the amphiphilic properties of the constituent molecules; they also have low interfacial tension with oil or aqueous carrier phases. Polymer solutions of long-chain polymers such as PNIPAm or polyurethane-polybutadienediol (pU-pBDO) can form excellent particles, but appear to be viscous and have significant viscoelastic response at the shear rates required for controlled droplet formation, thus significantly limiting the applicability. One-step double emulsification enables formation

http://dx.doi.org/10.5772/64521

of monodisperse particles from fluids that cannot normally be used in droplet-based microfluidics, including viscous or viscoelastic polymer solutions or low interfacial tension polymer melts. For example, a robust droplet formation mechanism has been proposed and demonstrated with highly viscous inner jet surrounded by a Newtonian fluid in one-step double emulsification, leading to formation of equal-sized droplets (see Figure 8) [61]. It takes long time for the droplet to relax into a spherical shape because of high viscosity of the fluid. The shape of droplet can be fixed by rapid solidification such as photoinduced cross-linking. This provides alternate approach to synthesize new types of particles, such as those made from waxy lipids or semidilute entangled polymer solutions.

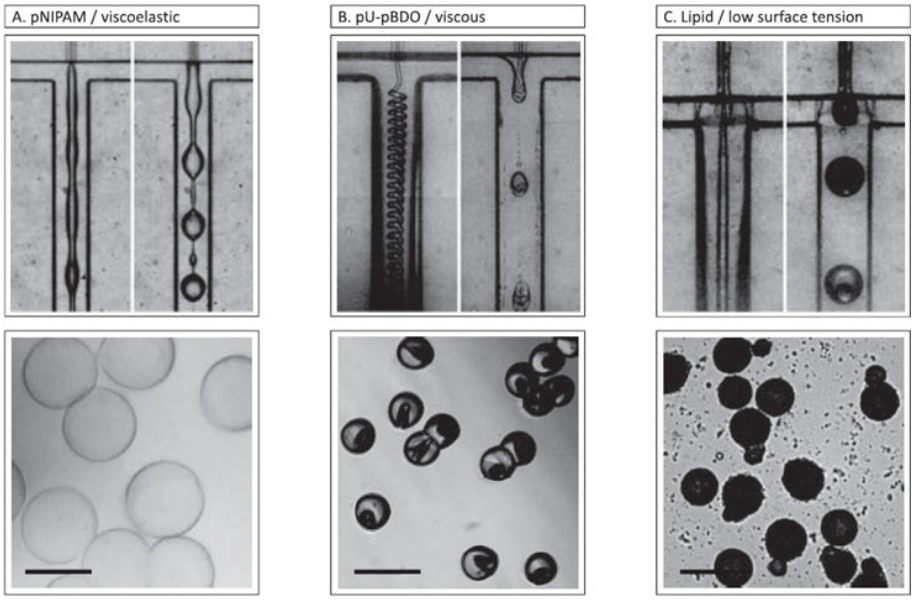

Figure 8. Demonstration of failing and succeeding emulsification using single- and one-step double emulsification, respectively. (a) Emulsification of a viscoelastic semidilute pNIPAM polymer solution and the resultant particles below. (b) Emulsification of a viscous and viscoelastic polymer solution composed of pU-pBDO and the resultant particles below. (c) Emulsification of a low interfacial tension and viscous lipid melt and the resultant particles below. All scale bars in the lower panels denote 100 μ m. Reprinted with permission from [61]. Copyright (2011) by Wiley-VCH Verlag GmbH & Co. KGaA, Weinheim.

5. Outlook

Functional materials such as microcapsules, microgels, colloidosomes, and microshells are ubiquitous in daily life and play crucial role in numerous industrial applications driven by microencapsulation. The materials can be obtained from the breakage of dispersed phase into droplets with controlled structure and monodispersed size in multiphase microsystem using emulsion as template. However, the practical applications of the technique are challenged as

the fluid precursors must be compatible with the formation of droplets in microfluidic devices. For instance, fluids with a low viscosity, negligible viscoelastic response, and moderate interfacial tension are required to facilitate formation of droplets. If even one of these constraints is not satisfied, polydisperse particles are formed or even jetting occurs. This may happen especially when one has to deal with biological fluids and polymeric solutions that contain molecules of high molecular weight. These complex fluids exhibit a non-Newtonian behavior which may considerably affect both the jetting/dripping transition and the growth of perturbations in the jetting regime. A number of novel approaches have been proposed in the last few years to fulfill research needs to achieve better control over drop size, degree of monodispersity, internal structure, and production rate. In this chapter, we have reviewed these novel microdroplet-based techniques when non-Newtonian fluids are involved. We focused on the synthesis of functional materials and how they can be linked with real industrial and biochemical demands. Despite of the rapid development, one of the major opened avenues for investigation is the material forming, through which one obtains a final solid phase, normally in the form of powders or suspensions made of microparticles, microcapsules, etc. More efforts should be given to the relevant research so that material forming can be carefully designed and well controlled to prevent unfavorable effects including coalescence, aggregation, or shell degradation and disintegration. Attention should also be paid to the development of advanced approach to inhibit the occurrence of satellite droplets and control polydispersity when non-Newtonian fluids are used in microfluidic system. This will eventually help to achieve applications such as advanced drug delivery.

Acknowledgements

This work was supported by Zhejiang Provincial Natural Science Foundation of China under Grant No. Q15E090001, Young Scientist Program from National Natural Science Foundation of China under Grant No. NSFC51506103/E0605, 2014 Zhejiang 1000-Talents Awards and Ningbo Natural Science Foundation under Grant No. 2015A610281.

Author details

Yong Ren[1*], Kai Seng Koh[2] and Yaping Zhang[3]

*Address all correspondence to: yong.ren@nottingham.edu.cn

1 Department of Mechanical, Materials and Manufacturing Engineering, The University of Nottingham Ningbo, China

2 Department of Chemical and Environmental Engineering, The University of Nottingham Ningbo, China

3 Department of Electrical and Electronic Engineering, The University of Nottingham Ningbo, China

References

[1] Schramm, L.L. (2005). Emulsions, Foams, and Suspensions: Fundamentals and Applications. Wiley-VCH, Germany.

[2] Mcclements, D.J. (2007). Critical review of techniques and methodologies for characterization of emulsion stability, Crit. Rev.Food Sci.Nutr. 47, 611–649.

[3] Budhian, A., Siegel, S.J., Winey, K.I. (2007). Haloperidol-loaded PLGA nanoparticles: systematic study of particle size and drug content, Int. J. Pharm. 336, 367–375.

[4] Berkland, C., King, M., Cox, A., Kim, K., Pack, D. (2002). Precise control of PLG microsphere size provides enhanced control of drug release date, J. Control. Release. 82, 137–147.

[5] Erb, R.M., Obrist, D., Chen, P.W., Studer, J., Studart, A.R. (2011). Predicting sizes of droplets made by microfluidic flow-induced dripping, Soft. Matter. 7, 8757–8761.

[6] Bird, R.B., Armstrong, R.C., Hassager, O. (1987). Dynamics of Polymeric Liquids. Volume 1: Fluid Mechanics, Wiley, USA.

[7] Larson, R.G. (1999). The Structure and Rheology of Complex Fluids. Oxford University Press, UK

[8] Rao, M.A. (2007). Rheology of Fluid and Semisolid Foods: Principles and Applications (2nd ed.). Springer. p. 8. ISBN 978-0-387-70929-1.

[9] Yang, S., Kim, J.Y., Lee, S.J., Lee, S.S., Kim, J.M. (2011). Sheathless elasto-inertial particle focusing and continuous separation in a straight rectangular microchannel, Lab. Chip. 11, 266–273.

[10] Derzsi, L., Kasprzyk, M., Plog, J.P., Garstecki, P. (2013). Flow focusing with viscoelastic liquids, Phys. Fluids, 25, 092001.

[11] Bird, R.B., Stewart, W.E., Lightfoot, E.N. (2002). Transport Phenomena, 2nd edition, Wiley, USA.

[12] Barnes, H.A., Hutton, J.F. and Walters, K. (1989). An Introduction to Rheology, Elsevier, Netherlands.

[13] Griskey, R.G., Nechrebecki, D.G., Notheis, P.J., Balmer, R.T. (1985). Rheological and pipeline flow behavior of corn starch dispersions, J. Rheol. 29, 349.

[14] Mujumdar, A., Beris, A.N., Metzner, A.B. (2002). Transient phenomena in thixotropic systems, J. Non-Newt. Fluid Mech., 102, 157–178.

[15] Rodd, L.E., Scott, T.P., Cooper-White, J.J., McKinley, G.H. (2005). Capillary breakup rheometry for low viscosity elastic fluids, Appl. Rheol. 15, 12–27.

[16] Shenoy, A.V. (1999). Rheology of Filled Polymer Systems, Springer, USA.

[17] Ren, Y., Liu, Z., Shum, H.C. (2015) Breakup dynamics and dripping-to-jetting transition in a shear-thinning/Newtonian multiphase microsystem, Lab. Chip. 15, 121–134.

[18] Roberts, C.C., Rao, R.R., Loewenberg, M., Brooks, C.F., Galambos, P., Grillet, A.M., Nemer, M.B. (2012). Comparison of monodisperse droplet generation in flow-focusing devices with hydrophilic and hydrophobic surfaces, Lab. Chip. 12, 1540–1547.

[19] Wang, K., Lu, Y.C., Xu, J.H., Tan, J., Luo, G.S. (2011). Generation of micromonodispersed droplets and bubbles in the capillary embedded T-junction microfluidic devices, J. AIChE. 57, 299–306.

[20] Couture, O., Faivre, M., Pannacci, N., Babataheri, A., Servois, V., Tabeling, P., Tanter, M. (2011). Ultrasound internal tattooing, Med. Phys. 38, 1116–1123.

[21] Utada, A.S., Fernandez-Nieves, A., Stone, H.A., Weitz, D.A. (2007). Dripping to jetting transition in coflow liquid streams, Phys. Rev. Lett. 99, 094502.

[22] Xu, J.H., Li, S.W., Tan, J., Luo, G.S. (2008). Correlations of droplet formation in T-junction microfluidic device: from squeezing to dripping, Microfluid. Nanofluid. 5, 711–717.

[23] Tice, J.D., Lyon, A.D., Ismagilov, R.F. (2004). Effects of viscosity on droplet formation and mixing in microfluidic channels, Anal. Chim. Acta. 507, 73–77.

[24] Oliveira, M.S.N., McKinley, G.H. (2005). Iterated stretching and multiple beads-on-a-string phenomena in dilute solutions of highly extensible flexible polymers, Phys. Fluids. 17, 071704.

[25] Eggers, J., Villermaux, E. (2008). Physics of liquid jets, Rep. Prog. Phys., 71, 036601.

[26] Stan, C.A., Tang, S.K.Y., Whitesides, G.M. (2009). Independent control of drop size and velocity in microfluidic flow-focusing generators using variable temperature and flow rate, Anal. Chem. 81, 2399–2402.

[27] Taylor, G.I. (1932). The viscosity of a fluid containing small drops of another fluid, Proc. R. Soc. London. A. 138, 41–48.

[28] Hong, Y., Wang, F. (2007). Investigation of viscosity effect on droplet formation, Microfluid. Nanofluid. 3, 341–346.

[29] Meier, M., Yadigaroglu, G., Smith, B.L. (2002). A novel technique for including surface tension in PLIC-VOF methods, Eur. J. Mech. B Fluids. 2, 61–73.

[30] Qiu, D.M., Silva, L., Tonkovich, A.L., Arora, R. (2010). Micro-droplet formation in non-Newtonian fluid in a microchannel, Microfluid. Nanofluid. 8, 531–548.

[31] Harvie, J.E., Davidson, M.R., Cooper-White, J.J., Rudman, M. (2007). A parametric study of droplet deformation through a microfluidic contraction: shear thinning liquids, Int. J. Multiphas. Flow. 33, 545–556.

[32] Tretheway, D.C., Leal, L.G. (2001). Deformation and relaxation of Newtonian drops in planar extensional flows of a Boger Fluid, J. Non-Newtonian Fluid Mech. 99, 81–108.

[33] Mason, T.G., Bibette, J. (1996). Emulsification in viscoelastic media. Phys. Rev. Lett. 77(16), 3481–3484.

[34] Husny, J., Cooper-White, J.J. (2006). The effect of elasticity on drop creation in T-shaped microchannels, J. Non-Newtonian Fluid Mech. 137, 121–136.

[35] Chung, C., Hulsen, M. A., Kim, J. M., Ahn, K. H., Lee, S.J. (2008). Numerical study on the effect of viscoelasticity on drop deformation in simple shear and 5:1:5 planar contraction/expansion microchannel, J. Non-Newtonian Fluid Mech. 155, 80–93.

[36] Love, J.C., Anderson, J.R., Whitesides, G.M. (2001). Fabrication of three-dimensional microfluidic systems by soft lithography, Mater. Res. Soc. July, 523–528.

[37] Chen, K.S., Ayon, A.A., Zhang, X., Spearing, S.M. (2002). Effect of process parameters on the surface morphology and mechanical performance of silicon structures after deep reactive ion etching (DRIE), J. Microelectromech. S. 11, 264–275.

[38] Zhang, J., Tan, K.L., Hong, G.D., Yang, L.J., Gong, H.Q. (2001). Polymerization optimization of SU-8 photoresist and its applications in microfluidic systems and MEMS, J. Micromech. Microeng. 11, 20–26.

[39] Reznikova, E.F., Mohr, J., Hein, H. (2005). Deep photo-lithography characterization of SU-8 resist layers, Microsys. Technol. 11, 282–291.

[40] Becker, H., Gärtnet, C. (2008). Polymer microfabrication technologies for microfluidic system, Anal. Bioanal. Chem. 390, 89–111.

[41] Marty, F., Rousseau, L., Saadany, B., Mercier, B., Francais, O., Mita, Y., Bourouina, T. (2005). Advanced etching of silicon based on deep reactive ion etching for silicon high aspect ratio microstructures and three-dimensional micro- and nanostructures, J. Microelectr. 36, 673–677.

[42] Kern, W., Puotinen, D.A. (1970). Cleaning solutions based on hydrogen peroxide for use in silicon semiconductor technology, Rca Rev. 31, 187–206.

[43] Labeed, F.H., Fatoyinbo, H.O. (2014). Microfluidics in detection science: lab-on-a-chip technologies, Eds. Cambridge: Royal Society of Chemistry, UK.

[44] Santana, P.P., Oliveira, I.M.F., Piccin, E. (2012). Evaluation of using Xurography as a new technique for the fabrication of disposable gold electrodes with high reproducible areas, Electrochem. Commun. 16, 96–99.

[45] Fouchal, F., Dickens, P. (2007). Adaptive screen printing for rapid manufacturing, Rapid Prototyping J. 13, 284–290.

[46] Cornelius, T.L. (2002). Computer Aided and Integrated Manufacturing Systems, Vol. 3: Optimization Methods, World Scientific, Singapore.

[47] Bartholomeusz, D.A., Boutté, R.W., Andrade, D. (2005). Xurography: rapid prototyping of microstructures using a cutting plotter, J. Microelectromechanical Syst. 14, 1364–1374.

[48] Chu, L.Y., Kim, J.W., Shah, R.K., Weitz, D.A. (2007). Monodisperse thermoresponsive microgels with tunable volume-phase transition kinetics, Adv. Funct. Mater. 17, 3499–3504.

[49] Shah, R.K., Kim, J.-W., Agresti, J.J., Weitz, D.A., Chu, L.-Y. (2008). Fabrication of monodisperse thermosensitive microgels and gel capsules in microfluidic devices, Soft Matter. 4, 2303–2309.

[50] Datta, S.S., Abbaspourrad, A., Amstad, E., Fan, J., Kim, S.H., Romanowsky, M., Shum, H.C., Sun, B., Utada, A.S., Windbergs, M., Zhou, S., Weitz, D.A. (2014). 25th anniversary article: double emulsion templated solid microcapsules: mechanics and controlled release, Adv. Mater. 26, 2205–2218.

[51] Shah, R.K., Kim, J-.W., Weitz, D.A. (2010). Monodisperse stimuli-responsive colloidosomes by self-assembly of microgels in droplets, Langmuir. 26, 1561–1565.

[52] Seiffert, S., Weitz, D.A. (2010). Controlled fabrication of polymer microgels by polymer-analogous gelation in droplet microfluidics, Soft Matter. 6, 3184–3190.

[53] Shum, H.C., Lee, D., Yoon, I., Kodger, T., Weitz, D.A. (2008). Double emulsion templated monodisperse phospholipid vesicles, Langmuir. 24, 7651–7653.

[54] Shum, H.C., Kim, J.-W., Weitz, D.A. (2008). Microfluidic fabrication of monodisperse biocompatible and biodegradable polymersomes with controlled permeability, J. Am. Chem. Soc. 130, 9543–9549.

[55] Kim, S.-H., Shum, H.C., Kim, J.W., Cho, J.-C., Weitz, D.A. (2011). Multiple polymersomes for programmed release of multiple components, J. Am. Chem. Soc. 133, 15165–15171.

[56] Nisisako, T., Okushima, S., Torii, T. (2005). Controlled formulation of monodisperse double emulsions in a multiple-phase microfluidic system, Soft Matter. 1, 23–27.

[57] Okushima, S., Nisisako, T., Torii, T., Higuchi, T. (2004). Controlled production of monodisperse double emulsions by two-step droplet breakup in microfluidic devices, Langmuir. 20, 9905–9908.

[58] Abate, A.R., Krummel, A.T., Lee, D., Marquez, M., Holtze, C., Weitz, D.A. (2008). Photoreactive coating for high-contrast spatial patterning of microfluidic device wettability, Lab Chip. 8, 2157–2160.

[59] Abate, A.R., Thiele, J., Weinhart, M., Weitz, D.A. (2010). Patterning microfluidic device wettability using flow confinement, Lab Chip. 10, 1774–1776.

http://dx.doi.org/10.5772/64521

[60] Abate, A.R., Weitz, D.A. (2009). High-order multiple emulsions formed in poly(dimethylsiloxane) microfluidics, Small. 5, 2030–2032.

[61] Abate, A.R., Kutsovsky, M., Seiffert, S., Windbergs, M., Pinto, L.F.V., Rotem, A., Utada A.S., Weitz, D.A. (2011). Synthesis of monodisperse microparticles from non-Newtonian polymer solutions with microfluidic devices, Adv. Mater. 23, 1757–1760.